catalysts

MDPI

Article

Insights into a Removal Mechanism of Triclosan Using an Electroactivated Persulfate-Coupled Carbon Membrane System

Junjing Li [1,*], Di Wu [1], Hongying Zhang [1], Liang Wang [1,2,*], Hong Wang [3] and Zhengchun Ba [4]

[1] School of Environmental Science and Engineering, Tiangong University, State Key Laboratory of Separation Membranes and Membrane Processes, Binshui West Road 399, Xiqing District, Tianjin 300387, China
[2] Membrane Technology Research Center, Cangzhou Institute of Tiangong University, East Side of No. 13 Fengtai Park, High-Tech District, Cangzhou 061019, China
[3] State Key Laboratory of Separation Membranes and Membrane Processes, National Center for International Joint Research on Separation Membranes, School of Materials Science and Engineering, Tiangong University, Tianjin 300387, China
[4] Qinghai Puzheng Industrial Waste Residue Development Co., Ltd., Ganhe Industrial Park, Huangzhong County, Xining 811605, China
* Correspondence: junjingli@tiangong.edu.cn (J.L.); mashi7822@163.com (L.W.)

Abstract: Triclosan (TCS), a broad-spectrum bacteriostatic agent with bactericidal and disinfectant properties, is one of the emerging pollutants of great interest. The electrically activated persulfate-coupled carbon membrane system was studied in this paper. The removal of triclosan achieved 90% within 40 min. Complete degradation can be achieved within 90 min. The electrode was characterized by scanning electron microscope (SEM) and X-ray photoelectron spectroscopy (XPS). The optimal reaction conditions were explored. The catalytic mechanism of the reaction was investigated. It was proved that hydroxyl radicals, sulfate radicals, and singlet oxygen were the main reactive oxygen species in the reaction process by the free radical quenching experiment and electron paramagnetic resonance spectrometer. The degradation path and mechanism of triclosan were investigated.

Keywords: advanced oxidation process; tubular carbon membrane; hydroxyl radical; singlet oxygen

check for updates

Citation: Li, J.; Wu, D.; Zhang, H.; Wang, L.; Wang, H.; Ba, Z. Insights into a Removal Mechanism of Triclosan Using an Electroactivated Persulfate-Coupled Carbon Membrane System. *Catalysts* **2023**, *13*, 1321. https://doi.org/10.3390/catal13101321

Academic Editor: Marta Pazos Currás

Received: 26 July 2023
Revised: 15 September 2023
Accepted: 18 September 2023
Published: 25 September 2023

Copyright: © 2023 by the authors. Licensee MDPI, Basel, Switzerland. This article is an open access article distributed under the terms and conditions of the Creative Commons Attribution (CC BY) license (https://creativecommons.org/licenses/by/4.0/).

1. Introduction

There are new pollutants, such as personal care products, that cause unavoidable pollution of the environment. They have been getting a lot of attention, and their treatment is therefore of increasing importance [1–5]. Triclosan (5-chloro-2-(2,4-dichlorophenoxy) phenol, TCS), as one of the emerging pollutants of high concern, is a broad-spectrum bacteriostatic agent with bactericidal and disinfectant properties. It was widely used in antibacterial soaps, deodorants, mouthwashes, toothpastes, cosmetics, and other personal hygiene products [6–8]. In recent years, due to the wider application of triclosan, it can be detected in municipal wastewater, surface water, and groundwater [9,10]. In Europe, at least 350 tons of TCS were discharged into the natural environment every year, and TCS accounted for 0.1~0.3% of the mass fraction of care products used per person each year [11–13]. In the United States, about 139 rivers have been tested, of which more than 112 rivers have been tested for excessive TCS content [14]. TCS is hydrophobic and lipophilic at the same time (logKow = 4.8 at pH = 7), with some accumulation in the biome [15–18]. The potential toxicity of TCS to organisms has been demonstrated in previous studies. According to reports, TCS can be transferred from birds to embryos and impact the health of offspring [19]. In addition, the presence of TCS in water can lead to the formation of chloroform and related trihalomethanes, as well as chlorinated dioxins produced by chlorine disinfection [20]. TCS has a high adsorption potential and easily precipitates in the environment due to its high octanol–water partition coefficient (logKow of 4.8) [15,16].

Persulfates (PS) have the ability to oxidize pollutants in water. Persulfates are water soluble and stable in water for months. PS ionizes in water to form more stable persulfate ($S_2O_8^{2-}$) with a longer half-life. Its oxidation reduction potential (E_0 = 2.01 V) is close to ozone (E_0 = 2.07 V) and higher than permanganate (E_0 = 1.7 V) and hydrogen peroxide (E_0 = 1.77 V). PS has high redox potential and contains O-O bonds, but it has a high bond energy (140 kJ/mol) and does not easily react directly with organic matter [21]. Persulfates activation is an advanced oxidation technique comparable to conventional Fenton reactions. When PS is activated, many reactive free radicals, such as hydroxyl radical ($^{\bullet}$OH), sulfate radical ($SO_4^{\bullet-}$), and singlet oxygen ($^1O_2$), are generated. These active species can degrade various aqueous organic pollutants. Compared with the Fenton reaction based on the $^{\bullet}$OH, the sulfate radical has a high redox potential (2.5~3.1 V) and is more stable than the $^{\bullet}$OH [22–24]. Due to their high redox potential, sulfate radicals can achieve the degradation of most of the pollutants in water [25,26]. As shown in previous studies, persulfate can be activated by heat, ultraviolet (UV), alkali, hydrogen peroxide, and transition metals [10,27,28]. In recent years, activated-persulfate-based advanced oxidation techniques have received increasing attention from researchers due to their high oxidative properties and non-selectivity for pollutants. The combined electrochemical and persulfate process for the treatment of pollutants has the advantages of a high removal rate, wide adaptability to external conditions, and a long half-life of the generated radicals [21]. In recent years, the commonly used electrochemical oxidation electrodes are mainly metal and metal oxide electrodes, diamond electrodes, and photochemical electrodes. Electroactivated persulfate degradation pollutants can achieve a higher removal rate. However, for electrically activated persulfate, limited mass transfer remains the main problem limiting the efficiency of the reaction. Although the catalyst can provide more active sites, the reaction often takes a long time for pollutant degradation due to mass transfer limitation, making it less efficient. In addition, the choice of electrode materials is another important factor limiting its reaction.

In order to overcome these problems, new materials and techniques have been developed to activate persulfates. Carbon material is a new type of heterogeneous activated persulfate catalyst. It has a large specific surface area and pore capacity, acid and base resistance, and a high utilization rate [29–31]. Carbon materials exist in the environment, such as activated carbon, biomass char, graphite, graphene, carbon nanotubes, etc. These carbon materials can activate persulfate due to the defects of carbon produced by sp^2/sp^3 hybrid carbon and the oxygen groups on their surface. It has been shown that the catalytic properties of carbon materials are related to the conformation, oxygen functional groups, degree of defects, and size structure of the pristine carbon [32,33]. Activation of persulfate by carbon-based catalysts generates both free and non-free radicals. Many carbon materials (such as biomass carbon, graphite, and graphene) themselves have low economic cost and rich resources, so they provide more possibilities and advantages in the selection of activated persulfate materials. In actual wastewater treatment, when considering the economic cost and the practicability of materials, the possibility of practical application is wider. Therefore, the use of carbon membrane as an electrode material coupled with electrochemical persulfate technology has largely solved the complex problems of electrode materials brought by previous researchers in the electroactivated persulfate process. The carbon membrane itself has a certain adsorption effect on pollutants, with a high specific surface area and high electronic conductivity, therefore, it is an electrode material more suitable for activating persulfates. During the reaction process of the electrochemically activated persulfate-coupled carbon membrane, due to the high specific surface area of the carbon membrane and its good conductivity, pollutants can be gathered on its surface, which can achieve better mass transfer. In addition, the addition of carbon and electricity can increase the possibility of activating persulfate, which can improve degradation efficiency, and it is expected to be able to efficiently remove traces of refractory organic pollutants in actual water bodies.

In this study, electroactivated persulfate-coupled carbon membrane system was constructed. The removal mechanism of triclosan in this system was investigated. Various characterization methods were used to characterize the tubular carbon membrane electrode. In order to study the activation of persulfate, quenching experiments and electron paramagnetic resonance (EPR) spectrometer characterization were conducted. The main active species in the reaction were studied. Furthermore, the degradation pathway of triclosan was investigated by liquid chromatography–tandem mass spectrometry (LC-MS/MS).

2. Results and Discussion

2.1. The Degradation of TCS

The degradation effect of TCS by the system of tubular carbon membrane/peroxydisulfate/electric was studied. For comparison, we also performed experiments on two systems: tubular carbon membrane/peroxydisulfate and tubular carbon membrane/electric. As shown in Figure 1a, the degradation of TCS in the three combined processes was very fast in the first 10 min, which was due to the fact that the membrane electrode in the combined process was made of carbon material, which had a certain adsorption effect [34,35]. However, the prepared carbon membrane electrode itself has pores, and there is an intra-pore diffusion pathway. Therefore, the dual effects of adsorption and intra-pore diffusion increased the mass transfer of the system. When using tubular carbon membrane/peroxydisulfate to degrade TCS, the degradation efficiency reached more than 80% in 90 min, from which it can be known that carbon-material-activated persulfate to degrade pollutants has a good degradation effect, which is in line with previous studies [36,37]. Additionally, the system of tubular carbon membrane/peroxydisulfate/electric had a higher removal efficiency under the same conditions, which can reach a removal efficiency of more than 90% within 90 min. TCS adsorption experiments showed that the tubular carbon film electrode has some adsorption capacity for TCS, but this was not its main role (Figure 1b). It suggested that the increased TCS degradation efficiency was not caused by adsorption but by the activation of peroxydisulfate (PDS). Compared with tubular carbon membrane/peroxydisulfate/electric processes, the other combined processes did not exhibit a better result. This was mainly because, firstly, the added PDS not only served as an electrolyte to facilitate electron transfer, but it can also be activated by the carbon material [38]. Secondly, this was also due to the adsorption of carbon materials and the presence of pores in the prepared carbon membrane electrodes themselves, and the presence of intra-pore diffusion pathways. Therefore, the dual effect of adsorption and intra-pore diffusion increased the mass transfer rate of the system, and the system was able to further improve the oxidative capacity of the system through the synergistic activation of peroxydisulfate by carbon materials and electrochemistry. From the scanning electron microscope images, it was clear that a large number of small fragments appeared on the surface of the membrane after the reaction (Figure 2b), compared with the one before the reaction (Figure 2a). This was due to the activation of persulfate in the carbon membrane, the reaction of the carbon material in certain pores, and the formation of small molecules after the degradation of the TCS, resulting in small fragments of the carbon membrane electrode.

2.2. Characterization of the Electrodes

To understand the basic structural properties of the tubular carbon membrane, the XPS, Raman, and SEM mapping of it were performed (Figure 3). As shown in the XPS, the main components of the tubular carbon membrane were carbon and minerals. According to previous studies, carbon materials had the ability to activate persulfate [33,38]. In addition, it has been reported that the presence of elemental nitrogen favors the generation of active sites for the activation of persulfate, and, depending on the type of nitrogen present, it favors the promotion of the oxidation process [39]. The common phenotypes of nitrogen present are pyridine nitrogen, pyrrole nitrogen, graphitic nitrogen, and nitrogen oxides, and the corresponding peak positions are 398 eV, 400 eV, 401 eV, and 403.3 eV. Whereas the presence of pyridine nitrogen is favorable for the generation of redox sites, the presence

of graphitic nitrogen is beneficial to the generation of activation sites, which are favorable for the activation of persulfate [40]. As can be seen in Figure 3b, it was found to be mainly composed of pyridine nitrogen and graphitic nitrogen. Further results of the split-peak plot showed that graphitic nitrogen dominated the content. Therefore, it was considered that the presence of nitrogen was likely to promote the activation of persulfate to produce sulphate radicals. Raman spectroscopy is mainly used to characterize the crystal structure, disorder, doping state, and defects of graphene-based materials [41]. The relative intensity of the peaks in the D band reflected the degree of disorder in the graphite crystal structure, with peaks located between 1200 and 1450 cm^{-1}. The peaks in the G band represent first-order scattered E2g vibrational modes to represent the sp^2 bonding structure of the carbon material, with peaks located between 1550 and 1600 cm^{-1}. The D/G intensity ratio is used to measure the disordered structure of graphite, and, in general, the larger the D/G ratio, the more obvious the nature of graphene's edges (e.g., defects, vacancies, etc.) [42]. The Raman spectrum in Figure 3c showed that the D peak (defective structure) of the tubular carbon film appeared at about 1361 cm^{-1} and the G peak (graphite structure) appeared at about 1600 cm^{-1}. The intensity ratio (I_D/I_G) of the tubular carbon membrane was 0.85, which was much higher than graphite (0.65), suggesting that more defective sites were formed and the sp^2 cluster number increased [43]. These results can prove the distribution of the main elements on the tubular carbon membrane and that it had more defect sites, which was conducive to the degradation of TCS. As shown in Figure 3d, the surface of the carbon membrane contains the elements C, N, O, S, and Cl, small amounts of Al and Si, which was consistent with the XPS results.

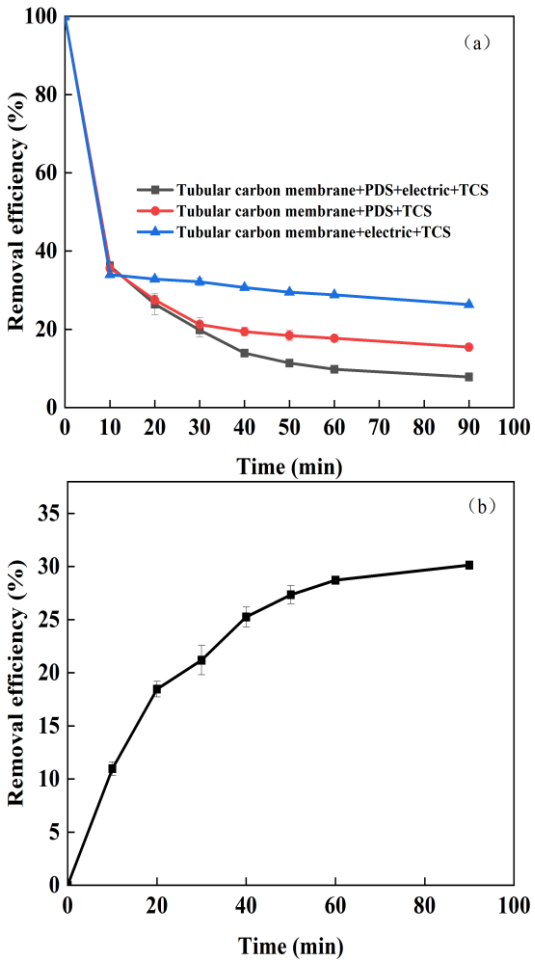


Figure 1. (**a**) Three combination modes on the TCS removal efficiency. (**b**) Effect of adsorption on degradation: $[TCS]_0$ = 5 mg·L^{-1}; $[PDS]_0$ = 20 mg·L^{-1}; $[electric]_0$ =2 V; pH = 7.0.

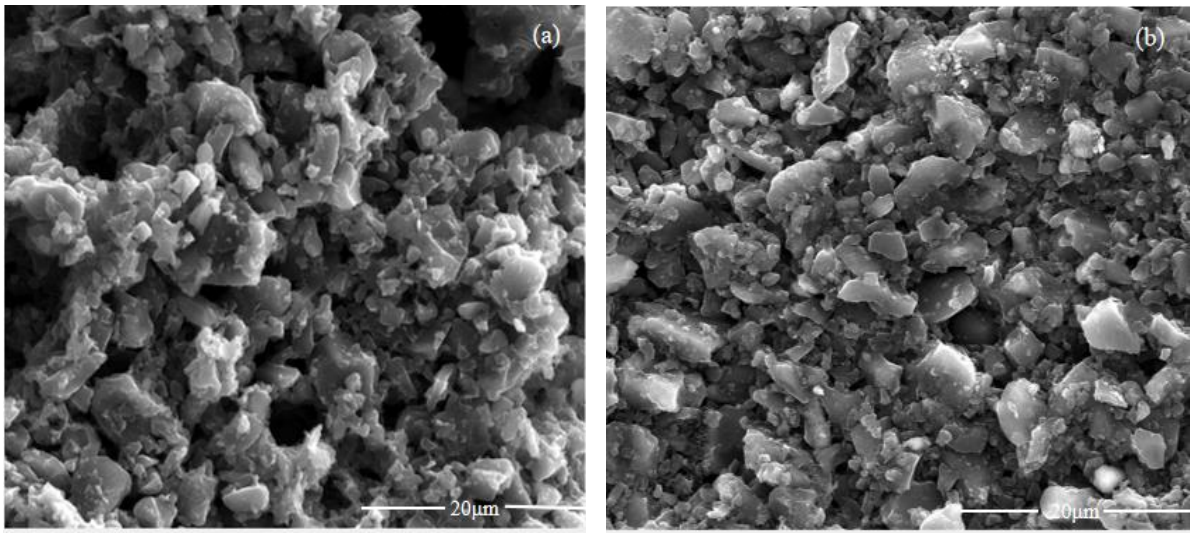


Figure 2. SEM images of the carbon membrane surface: (**a**) before reaction, (**b**) after the reaction.

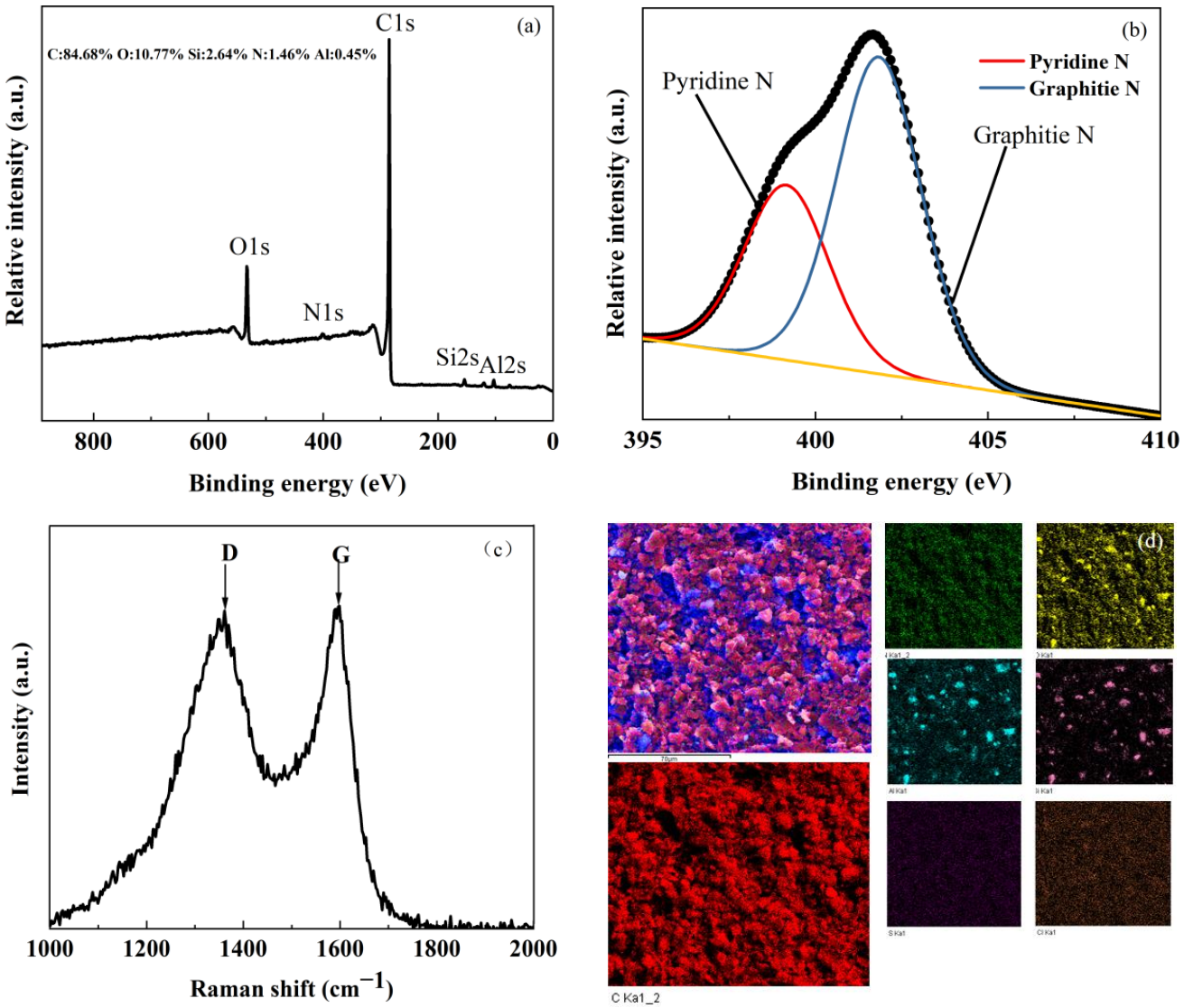


Figure 3. (**a**,**b**) XPS survey. (**c**) Raman spectra of tubular carbon membrane. (**d**) The SEM mapping image of tubular carbon membrane.

2.3. Free Radical Recognition

Activation of PS has been reported to generate $SO_4^{\bullet-}$, and $SO_4^{\bullet-}$ can further react with H_2O to form $^{\bullet}OH$ [44]. In this work, the EPR spin-trapping technique using 5,5-Dietyl-1-pyrroline-N-oxide (DMPO) and 2,2,6,6-Tetramethylpiperidine-1-oxylwere (TEMP) was used to identify the radical species generated by the tubular carbon membrane/PDS/electric systems (Figure 4). The reaction solution at 10 min and 40 min in the reaction process was drawn for the detection and the signal of free radicals. It can be determined that the reactive oxygen species were $SO_4^{\bullet-}$, $^{\bullet}OH$, and $^1O_2$ [45,46]. It was found that the signal generated by free radicals and non-radicals in 40 min was stronger than that in 10 min. At the same time, the contribution of singlet oxygen played a major role, which showed that as the reaction time increased, the accumulation of free radicals and non-radicals was increased.

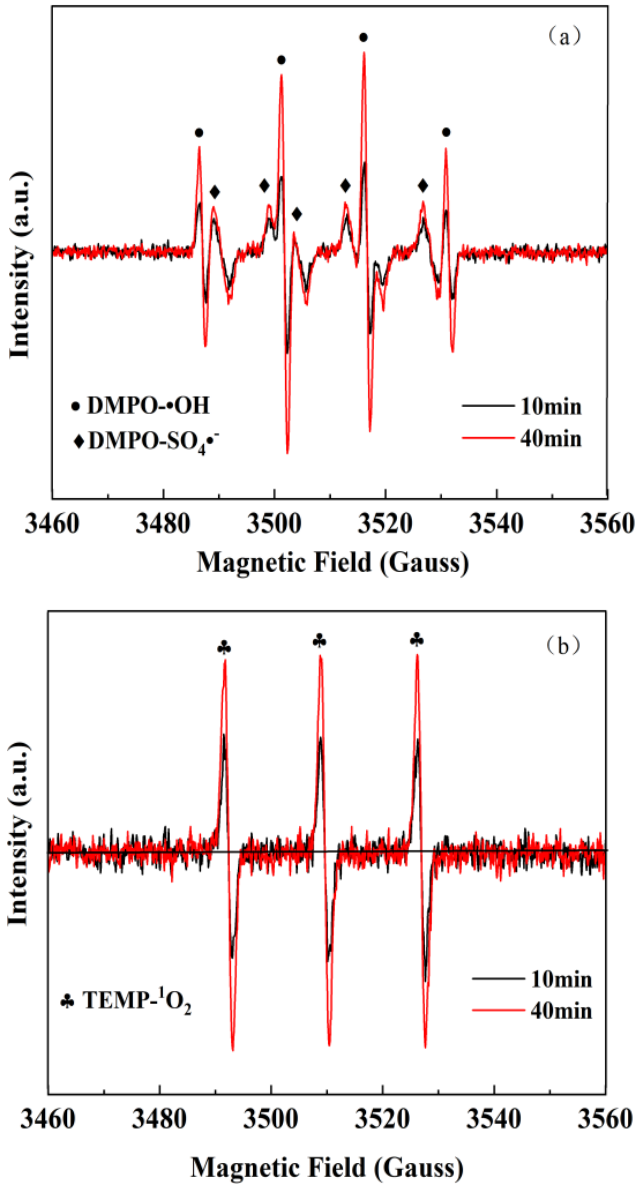


Figure 4. EPR spectra obtained by spin-trapping with (**a**) DMPO and (**b**) TEMP in the presence of the tubular carbon membrane/PDS/electric system: $[TCS]_0$ = 5 mg·L^{-1}; $[PDS]_0$ = 20 mg·L^{-1}; $[DMPO]_0$ = 200 mM; $[TEMP]_0$ = 80 mM; pH = 7.0.

2.4. Effects of Radical Scavengers

In order to investigate the degradation of TCS by a tubular carbon membrane coupled with an electrochemically activated persulfate system, free radical quenching experiments were carried out (Figure 5). It is reported that methanol has a strong quenching effect on both $SO_4^{\bullet-}$ and $^{\bullet}OH$, and tert-butanol has a strong quenching effect on $^{\bullet}OH$ and a weak quenching effect on $SO_4^{\bullet-}$. Therefore, $SO_4^{\bullet-}$ and $^{\bullet}OH$ in the system can be distinguished by methanol and tert-butanol. Tert-butanol was used as a free radical scavenger for $^{\bullet}OH$ [47], and furfuryl alcohol was used as scavenger for singlet oxygen ($^1O_2$) [48,49]. It is shown in Figure 4 that during the reaction process, furfuryl alcohol, tert-butanol, and methanol, respectively, inhibited the degradation of TCS, which resulted in the removal efficiency reaching about 45%, 25%, and 15%, indicating that the reactive oxygen species were mainly $SO_4^{\bullet-}$, $^{\bullet}OH$, and $^1O_2$. According to the above results, it can be determined that the reaction involves both free radicals and non-radicals.

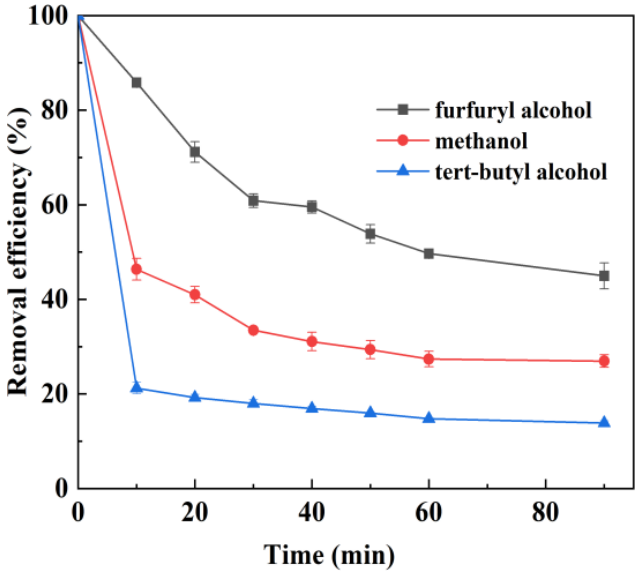


Figure 5. Degradation of TCS by the tubular carbon membrane/PDS/electric system with radical scavengers: $[TCS]_0$ = 5 mg·L^{-1}; $[PDS]_0$ = 20 mg·L^{-1}; $[Methanol]_0$ = 0.5 M; $[Furfuryl\ alcohol]_0$ = 0.5 M; $[Tert\text{-}butanol]_0$ = 0.5 M; pH = 7.0.

2.5. PDS Concentration, Cycle Pump Flow Rate, and pH Impact

The effect of the PDS concentration and the flow rate of the cycle pump on TCS degradation was investigated. In Figure 6a, when the PDS concentration was 10 mg·L^{-1}, the removal efficiency was 71%. This was mainly because the reduced $SO_4^{\bullet-}$ production failed to fully oxidize the target pollutant. As the initial PDS increased, more $SO_4^{\bullet-}$ would participate in the oxidation reaction, so that the removal efficiency of TCS was significantly increased [50,51]. When the concentration was further increased, the degradation efficiency of TCS was not significantly increased, due to excessive $SO_4^{\bullet-}$ self-reaction or self-quenching reaction with excess PDS, according to Equations (1) and (2). This phenomenon demonstrated that there was more $SO_4^{\bullet-}$ production, but it was not involved in the oxidation reaction [52].

$$SO_4^{\bullet-} + SO_4^{\bullet-} \rightarrow S_2O_8^{2-} \quad (1)$$

$$SO_4^{\bullet-} + S_2O_8^{2-} \rightarrow SO_4^{2-} + S_2O_8^{\bullet-} \quad (2)$$

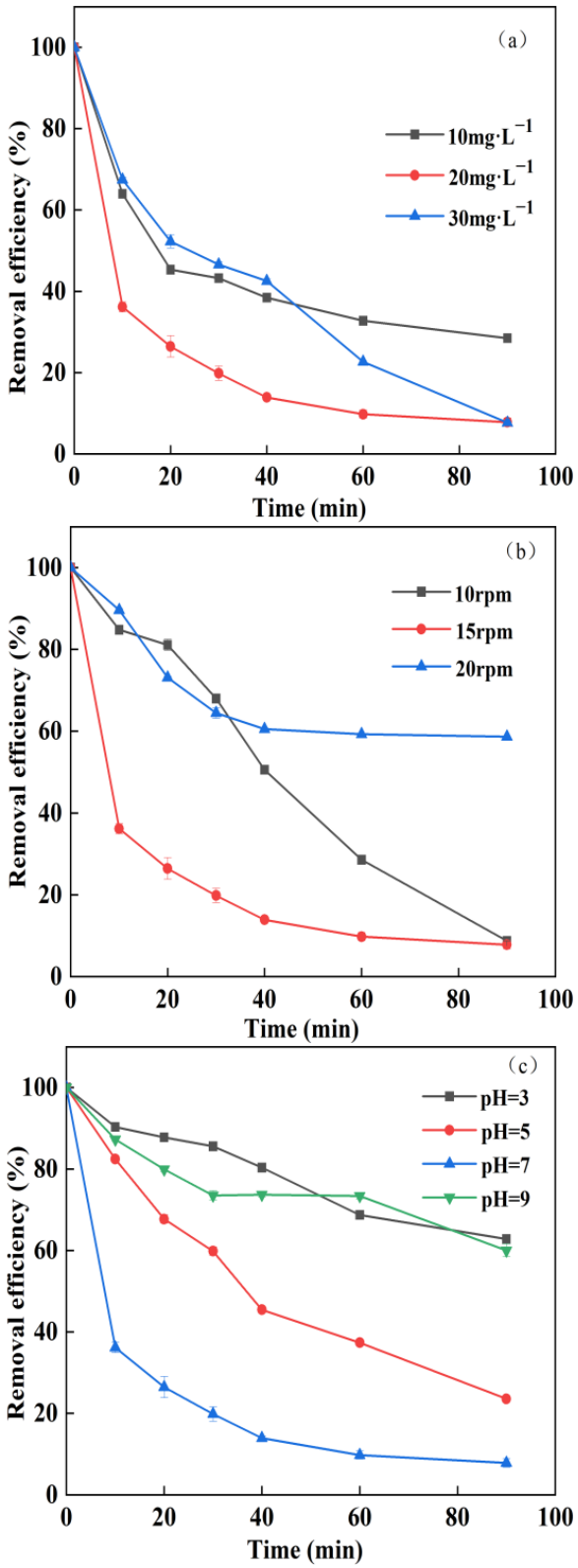


Figure 6. Degradation of TCS by the tubular carbon membrane/PDS/electric system with radical scavengers, with respect to (**a**) PDS concentration, (**b**) speed of revolution, (**c**) pH: $[TCS]_0$ = 5 mg·L^{-1}.

In Figure 6b, when the rotation speed increased from 10 to 15 rpm, the final removal efficiency was not improved, and the removal efficiency in the interval time was not as high as that of 10 rpm. This is attributed to the fact that increasing the rotational speed of

the circulating pump can further promote the mass transfer of the system. Meanwhile, the high mass transfer would cause TCS to occupy part of the active site, leading to slower efficiency. When the speed reached 20 rpm, this resulted in some contaminants entering the effluent vessel directly with the PDS without having time to react, resulting in a removal efficiency of only 41%.

The pH is an important factor influencing the free radical production and degradation effect during the PDS activation process [53,54]. Therefore, the initial pH was adjusted to values of 3, 5, 7, and 9, respectively. In Figure 6c, the degradation efficiency continuously increases from 37% to the maximum as the pH increases from 3 to 7. Under acidic conditions, more H^+ ions will remove the resulting $SO_4^{\bullet -}$ and $^{\bullet}OH$, limiting the removal efficiency [55]. Under alkaline conditions, on the one hand, the adsorption capacity of carbon materials for TCS was weakened. On the other hand, degradation of TCS by sulfate radicals was reduced. In the meantime, the existence time of the hydroxyl radical was shorter than that of the sulfate radical, and the mass transfer effect was not as good as that of the sulfate radical. Therefore, TCS removal was less effective under alkaline conditions. In conclusion, the best removal efficiency was achieved in neutral conditions [53].

2.6. Proposed Mechanism for the Removal of TCS

In this study, it was found that the carbon-membrane-coupled electric field exhibited high catalytic activity toward PDS decomposition for TCS degradation. Therefore, identifying the substances involved in the reaction process will help to better understand the degradation pathways. The solution of TCS was chosen as simulated wastewater to study the degradation process in the present system with a voltage of 2 V.

The degradation products of triclosan were analyzed by negative ion mode electrospray mass spectrometry (-ESI-MS), and the structure of the degradation products was determined according to the obtained mass spectra. The initial substrate was triclosan (deprotonated quasi-molecular ion peak $[M]^+$ m/z 287 obtained by ionization in electrospray mass spectrometry). When the degradation reaction occurred, the main degradation site occurred on the benzene ring in the molecular structure. On the benzene ring in the structure, there were two main degradation reaction pathways: hydroxylation and dechlorination. The first degradation reaction path is the cleavage of the C_{sp2}–O bond connecting the benzene ring. The m/z 143 and m/z 161 are obtained, respectively. The latter is oxidized, which obtained the hydroxylated products of the benzene ring m/z 177 and m/z 193. The second degradation reaction pathway is represented by the continuous removal of chlorine atoms from the benzene ring and the oxidative hydroxylation process to obtain the initial intermediate products m/z 269, m/z 251, and m/z 233. Dechlorination was mainly due to electron transfer induced by sulfate radicals [56]. In addition, electron transfer can form carbon-centred radicals in the benzene ring, thus inducing hydroxylation in the benzene ring [57]. The further degradation of the above products is proved by the oxidative ring opening of the benzene ring. The further decarboxylation and the decarboxylation and reoxidation correspond to three paths, respectively: the degradation products m/z 275, m/z 231, m/z 205, and m/z 187; the degradation products m/z 257, m/z 213, and m/z 187; and the degradation products m/z 239, m/z 195, m/z 169, etc. From the product m/z 233, ring cracking can occur to obtain m/z 195. In addition, m/z 195 can be obtained from the product m/z 233 by ring cracking.

The further degradation of the above products showed the oxidative ring opening of the ring to obtain products, such as m/z 131 and m/z 133, which further degrade to produce small molecules of carboxylic acid and that finally degrade to obtain H_2O, CO_3^{2-}, Cl^-, etc. (Figure 7).

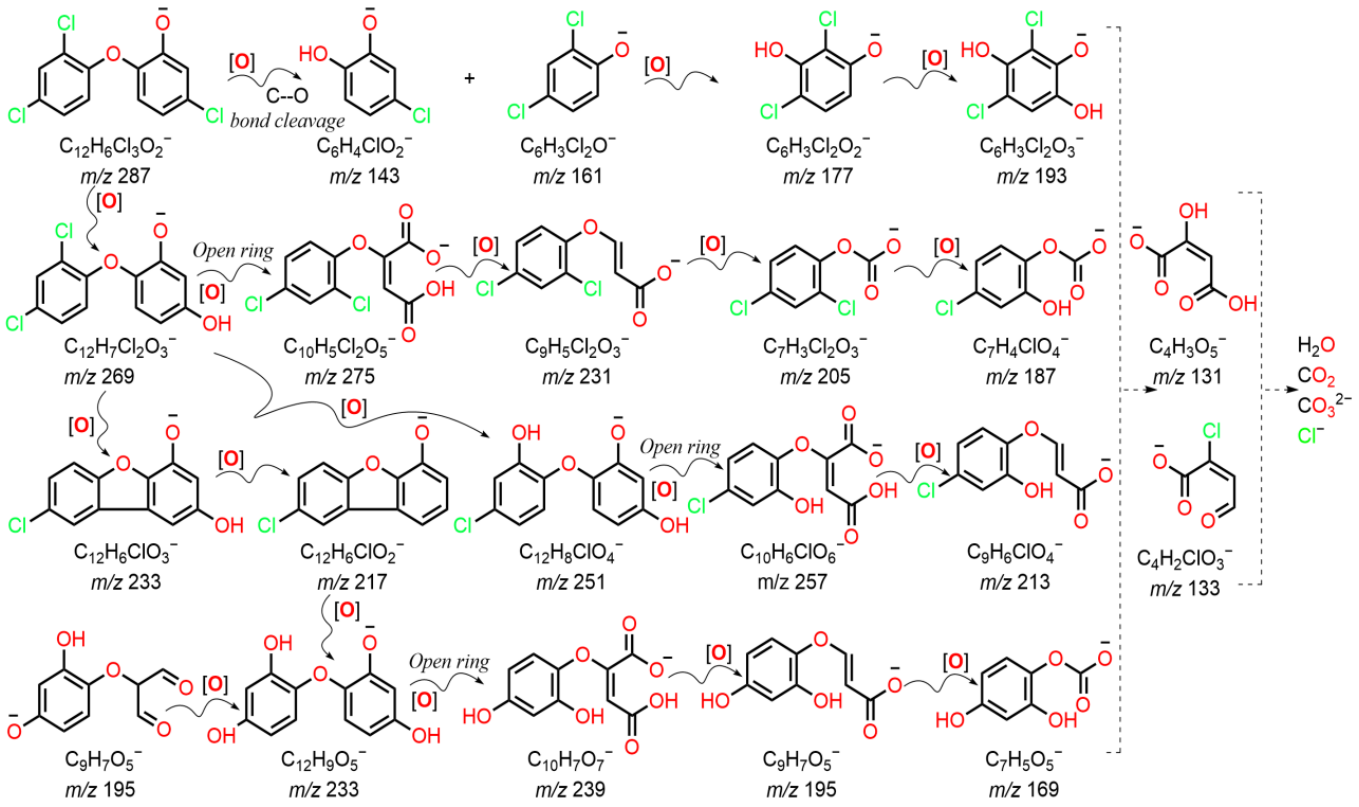


Figure 7. Degradation pathways and mechanism of triclosan.

3. Materials and Methods

3.1. Chemicals

Triclosan (97%), furfuryl alcohol, and tert-butyl alcohol were obtained from Shanghai Macklin Biochemical Bechnology Co., Ltd. (Shanghai, China). Potassium peroxodisulfate was provided by Tianjin Beilian Fine Chemicals Development Co., Ltd. (Tianjin, China). HPLC-grade methanol (MeOH) was used for sample analyses provided by Tianjin North Tianyi Chemical Reagent Factory (Tianjin, China). All chemicals were of analytical grade or higher and used as received without further purification. Deionized water was used in all experiments.

3.2. Preparation of Carbon Membrane Electrode

Tubular carbon membranes (1 cm in diameter) were used for preparing the desired electrodes. The tubular carbon membrane was cut into 7 cm long sections, rinsed with deionized water and sonicated for 30 min, and then soaked in concentrated hydrochloric acid for 24 h to remove surface impurities. Then, it was rinsed with deionized water until it was neutral and put in an oven to dry. Both ends of the dried tubular carbon membrane were sealed with epoxy resin and used as a carbon membrane electrode.

3.3. Degradation Experiments

An electrically activated persulfate-coupled carbon membrane reaction was performed at room temperature (20 ± 2 °C) in a single-chamber reactor (length 20 cm, 5 cm diameter) made of quartz glass material. A tubular carbon membrane (length 7 cm) electrode was used as the anode and a stainless steel mesh electrode was used as the cathode. The stainless steel mesh surrounded the tubular carbon membrane, and the distance between the stainless steel mesh and the tubular carbon membrane was 2.5 cm. The electrode assembly was connected to a DC power supply (DJS-292C, Shanghai Xinrui Instrument Co., Ltd., Shanghai, China). The voltage used for the experiment was a constant voltage of 2 V.

The concentration of triclosan was 5 mg·L^{-1}. The concentration of potassium persulfate was 20 mg·L^{-1}. Samples were extracted at predetermined intervals during the 90 min reaction using 1 mL syringes and immediately filtered using 0.22 μm polytetrafluoroethylene syringe filters. The whole experiment was repeated three times.

3.4. Analytical Methods

The TCS concentration was measured using high-performance liquid chromatography (HPLC, Shimadzu Corporation, Kyoto, Japan) with a UV detector wavelength of 282 nm equipped with a C18 column (5 μm, 4.6 × 250 mm). The mobile phase was a methanol/water mixture (80%/20%, *v/v*) with a flow rate of 1 mL·min $^{-1}$ and a sample volume of 20 μL with a column temperature of 40 °C. Intermediate products were identified using a liquid chromatography–tandem mass spectrometry (LC-MS/MS) system (Waters I/Xevo G2Q-Tof, Waters, Milford, MA, USA) with a C18 column (1.8 μm, 2.1 × 50 mm). The active ingredients produced during the potassium peroxodisulfate activation process were detected using electron paramagnetic resonance. DMPO was used to capture radicals ($SO_4^{\bullet -}$ and $^{\bullet}OH$) and TEMP was used to capture singlet oxygen. The instrument was set to a microwave frequency of 9.77 GHz, with a center field of 3498.68 G, a scan width of 100 G, and a modulation amplitude of 1 G.

4. Conclusions

In this study, an electroactivated persulfate-coupled carbon membrane system was constructed. The tubular carbon membrane/peroxydisulfate/electrochemical system achieved more than 90% degradation of TCS within 90 min. The results showed that electrolysis had a synergistic effect with the activation of persulfate by carbon materials. The adsorption of carbon materials as well as the prepared carbon membrane electrodes themselves had pores, and there was an intra-pore diffusion pathway. Thus, the dual effect of adsorption and intra-pore diffusion increased the mass transfer capacity of the system and therefore further improved the oxidative capacity of the system. In this case, appropriate operating conditions favored the synergistic process and could promote the degradation of TCS. The optimized conditions were as follows: a PDS dose of 20 mg L^{-1}; an applied voltage of 2 V; an initial pH of 7; and a cycle pump flow rate of 15 rpm. The triclosan degradation mechanism was proposed based on the LC-MS analysis. EPR results confirmed the formation of sulfate radical anions ($SO_4^{\bullet -}$), hydroxyl radical ($^{\bullet}OH$), and singlet oxygen ($^1O_2$) in PDS activation.

This study contributed to a better understanding of the interaction between carbon materials and combined electrochemical and membrane technologies and provided potential strategies for wastewater treatment based on persulfate activation.

Author Contributions: J.L.: Conceptualization, Review and revision; D.W.: Data curation, Writing—Original draft preparation; H.Z.: Data curation, Methodology, Writing—Original draft preparation; L.W.: Supervision; H.W.: Formal analysis; Z.B.: Formal analysis. All authors have read and agreed to the published version of the manuscript.

Funding: China Postdoctoral Science Foundation: 2020T130470; China Postdoctoral Science Foundation: 2018M641656; the research funding provided by Cangzhou Institute of Tiangong University: Grant No. TGCYY-Z-0101; TGU Grant for Fiber Studies: TGF-21-B3.

Data Availability Statement: All relevant data are within the paper.

Acknowledgments: We would like to thank the Analytical & Testing Center of Tiangong University for X-ray photoelectron spectroscopy.

Conflicts of Interest: The authors declare no competing financial interests.

References

1. Cantwell, M.G.; Katz, D.R.; Sullivan, J.C.; Shapley, D.; Lipscomb, J.; Epstein, J.; Juhl, A.R.; Knudson, C.; O'Mullan, G.D. Spatial Patterns of Pharmaceuticals and Wastewater Tracers in the Hudson River Estuary. *Water Res.* **2018**, *137*, 335–343. [CrossRef] [PubMed]
2. Li, J.J.; Wang, Y.; Zhao, B.; Ding, J.; Zhang, J.; Yin, M.H.; Zhang, Z.H.; Ma, S.M.; Liu, Y.Q.; Tan, Z.L. Unraveling Kinetics and Mechanism of Electrocatalytic Hydrodechlorination of Chlorinated PPCPs by Nickel-Cobalt Metal Organic Framework Supported Palladium Composite Electrode. *Appl. Catal. B Environ.* **2023**, *332*, 122754. [CrossRef]
3. Li, J.J.; Kong, K.Z. Efficient Palladium Catalysts: Application and Challenges of Electrocatalytic Hydrodechlorination Technology in Wastewater Treatment. *ChemCatChem* **2023**, e202300908. [CrossRef]
4. Qi, Y.M.; Zou, M.T.; Ajarem, J.S.; Allam, A.A.; Wang, Z.Y.; Qu, R.J.; Zhu, F.; Huo, Z.L. Catalytic Degradation of Pharmaceutical and Personal Care Products in Aqueous Solution by Persulfate Activated with Nanoscale FeCoNi-ternary Mixed Metal Oxides. *Sep. Purif. Technol.* **2023**, *314*, 123585. [CrossRef]
5. Li, J.J.; Ma, S.M.; Qi, Z.Y.; Ding, J.; Yin, M.H.; Zhao, B.; Zhang, Z.H.; Wang, Y.; Zhang, H.W.; Wang, L. Insights into the Removal of Chloramphenicol by Electrochemical Reduction on Pd/NiFe-MOF/foam-Ni Electrode: Performance and Mechanism. *Appl. Catal. B Environ.* **2023**, *322*, 122076. [CrossRef]
6. Chen, X.J.; Richard, J.; Liu, Y.L.; Dopp, E.; Tuerk, J.; Bester, K. Ozonation Products of Triclosan in Advanced Wastewater Treatment. *Water Res.* **2012**, *46*, 2247–2256. [CrossRef] [PubMed]
7. Gao, H.P.; Chen, J.B.; Zhang, Y.L.; Zhou, X.F. Sulfate Radicals Induced Degradation of Triclosan in Thermally Activated Persulfate System. *Chem. Eng. J.* **2016**, *306*, 522–530. [CrossRef]
8. Cai, S.; Hu, X.X.; Lu, D.; Zhang, L.; Jiang, C.L.; Cai, T.M. Ferrous-Activated Persulfate Oxidation of Triclosan in Soil and Groundwater: The Roles of Natural Mineral and Organic Matter. *Sci. Total Environ.* **2021**, *762*, 143092. [CrossRef]
9. Quan, B.Y.; Li, X.; Zhang, H.; Zhang, C.; Ming, Y.; Huang, Y.C.; Xi, Y.N.; Xu, W.H.; Liu, Y.G.; Tang, Y.Q. Technology and Principle of Removing Triclosan from Aqueous Media: A Review. *Chem. Eng. J.* **2019**, *378*, 122185. [CrossRef]
10. Li, J.J.; Liang, Y.Q.; Jin, P.L.; Zhao, B.; Zhang, Z.H.; He, X.J.; Tan, Z.L.; Wang, L.; Cheng, X.W. Heterogeneous Metal-Activated Persulfate and Electrochemically Activated Persulfate: A Review. *Catalysts* **2022**, *12*, 1024. [CrossRef]
11. Sabaliunas, D.; Webb, S.F.; Hauk, A.; Jacob, M.; Eckhoff, W.S. Environmental Fate of Triclosan in the River Aire Basin, UK. *Water Res.* **2003**, *37*, 3145–3154. [CrossRef] [PubMed]
12. Schweizer, H.P. Triclosan: A Widely Used Biocide and Its Link to Antibiotics. *FEMS Microbiol. Lett.* **2001**, *202*, 1–7. [CrossRef] [PubMed]
13. Singer, H.; Muller, S.; Tixier, C.; Pillonel, L. Triclosan: Occurrence and Fate of a Widely Used Biocide in the Aquatic Environment: Field Measurements in Wastewater Treatment Plants, Surface Waters, and Lake Sediments. *Environ. Sci. Technol.* **2002**, *36*, 4998–5004. [CrossRef] [PubMed]
14. Perez, A.L.; De Sylor, M.A.; Slocombe, A.J.; Lew, M.G.; Unice, K.M.; Donovan, E.P. Triclosan Occurrence in Freshwater Systems in the United States (1999-2012): A Meta-Analysis. *Environ. Toxicol. Chem.* **2013**, *32*, 1479–1487. [CrossRef] [PubMed]
15. Wang, Y.W.; Liang, W. Occurrence, Toxicity, and Removal Methods of Triclosan: A Timely Review. *Curr. Pollut. Rep.* **2021**, *7*, 31–39. [CrossRef]
16. Chen, Y.; Fang, J.Z.; Ren, L.; Fan, R.F.; Zhang, J.Q.; Liu, G.H.; Zhou, L.; Chen, D.Y.; Yu, Y.X.; Lu, S.Y. Urinary Bisphenol Analogues and Triclosan in Children from South China and Implications for Human Exposure. *Environ. Pollut.* **2018**, *238*, 299–305. [CrossRef]
17. Kalloo, G.; Wellenius, G.A.; McCandless, L.; Calafat, A.M.; Sjodin, A.; Karagas, M.; Chen, A.M.; Yolton, K.; Lanphear, B.P.; Braun, J.M. Profiles and Predictors of Environmental Chemical Mixture Exposure among Pregnant Women: The Health Outcomes and Measures of the Environment Study. *Environ. Sci. Technol.* **2018**, *52*, 10104–10113. [CrossRef]
18. Lu, S.Y.; Wang, N.; Ma, S.T.; Hu, X.; Kang, L.; Yu, Y.X. Parabens and Triclosan in Shellfish from Shenzhen Coastal Waters: Bioindication of Pollution and Human Health Risks. *Environ. Pollut.* **2019**, *246*, 257–263. [CrossRef]
19. Possenti, C.D.; Poma, G.; Defosse, S.; Caprioli, M.; De Felice, B.; Romano, A.; Saino, N.; Covaci, A.; Parolini, M. Embryotoxic Effects of In-ovo Triclosan Injection to the Yellow-Legged Gull. *Chemosphere* **2019**, *218*, 827–835. [CrossRef]
20. Dhillon, G.S.; Kaur, S.; Pulicharla, R.; Brar, S.K.; Cledon, M.; Verma, M.; Surampalli, R.Y. Triclosan: Current Status, Occurrence, Environmental Risks and Bioaccumulation Potential. *Int. J. Environ. Res. Public Health* **2015**, *12*, 5657–5684. [CrossRef]
21. Wang, B.W.; Wang, Y. A comprehensive Review on Persulfate Activation Treatment of Wastewater. *Sci. Total Environ.* **2022**, *831*, 154906. [CrossRef] [PubMed]
22. Huang, K.C.; Couttenye, R.A.; Hoag, G.E. Kinetics of Heat-Assisted Persulfate Oxidation of Methyl Tert-butyl Ether (MTBE). *Chemosphere* **2002**, *49*, 413–420. [CrossRef]
23. Cong, J.; Wen, G.; Huang, T.L.; Deng, L.Y.; Ma, J. Study on Enhanced Ozonation Degradation of Para-Chlorobenzoic Acid by Peroxymonosulfate in Aqueous Solution. *Chem. Eng. J.* **2015**, *264*, 399–403. [CrossRef]
24. Neta, P.; Huie, R.E.; Ross, A.B. Rate Constants for Reactions of Inorganic Radicals in Aqueous Solution. *J. Phys. Chem. Ref. Data* **1988**, *17*, 1027–1284. [CrossRef]
25. Liu, M.J.; Liu, Y.; Liu, X.R.; Chu, C.C.; Yao, D.C.; Mao, S. Peroxydisulfate Activation by 2D MOF-derived Ni/Fe_3O_4 Nanoparticles Decorated in 3D Graphene Oxide Network. *Sep. Purif. Technol.* **2022**, *301*, 121967. [CrossRef]
26. Qiu, H.B.; Guo, P.C.; Yuan, L.; Sheng, G.P. Different Non-Radical Oxidation Processes of Persulfate and Peroxymonosulfate Activation by Nitrogen-doped Mesoporous Carbon. *Chin. Chem. Lett.* **2020**, *31*, 2614–2618. [CrossRef]

27. Dubois, V.; Rodrigues, C.S.D.; Alves, A.S.P.; Madeira, L.M. UV/Vis-Based Persulphate Activation for p-Nitrophenol Degradation. *Catalysts* **2021**, *11*, 480. [CrossRef]
28. Li, Z.D.; Sun, Y.M.; Liu, D.F.; Yi, M.L.; Chang, F.; Li, H.T.; Du, Y.Y. A Review of Sulfate Radical-Based and Singlet Oxygen-Based Advanced Oxidation Technologies: Recent Advances and Prospects. *Catalysts* **2022**, *12*, 1092. [CrossRef]
29. Lu, K.; Min, Z.; Qin, J.; Shi, P.; Wu, J.; Fan, J.; Min, Y.; Xu, Q. Preparation of Nitrogen Self-Doped Hierarchical Porous Carbon with Rapid-Freezing Support for Cooperative Pollutant Adsorption and Catalytic Oxidation of Persulfate. *Sci. Total Environ.* **2021**, *752*, 142282. [CrossRef]
30. Li, Z.L.; Cao, D.; Cheng, H.; Chen, F.; Nan, J.; Liang, B.; Sun, K.; Huang, C.; Wang, A.J. Ordered Mesoporous Carbon as An Efficient Heterogeneous Catalyst to Activate Peroxydisulfate for Degradation of Sulfadiazine. *Chin. Chem. Lett.* **2022**, *33*, 2747–2752. [CrossRef]
31. Lan, R.J.; Su, W.B.; Li, J.T. Preparation and Catalytic Performance of Expanded Graphite for Oxidation of Organic Pollutant. *Catalysts* **2019**, *9*, 280. [CrossRef]
32. Gao, Y.; Wang, Q.; Ji, G.Z.; Li, A.M. Degradation of Antibiotic Pollutants by Persulfate Activated with Various Carbon Materials. *Chem. Eng. J.* **2022**, *429*, 132387. [CrossRef]
33. Liang, J.; Chen, K.X.; Duan, X.G.; Zhao, L.; Qiu, H.; Xu, X.Y.; Cao, X.D. pH-Dependent Generation of Radical and Nonradical Species for Sulfamethoxazole Degradation in Different Carbon/Persulfate Systems. *Water Res.* **2022**, *224*, 119113. [CrossRef] [PubMed]
34. Yang, G.C.C.; Yen, C.H. The Use of Different Materials to form the Intermediate Layers of Tubular Carbon Nanofibers/Carbon/Alumina Composite Membranes for Removing Pharmaceuticals from Aqueous Solutions. *J. Membr. Sci.* **2013**, *425*, 121–130. [CrossRef]
35. Nimai, S.L.; Zhang, H.; Wu, Z.L.; Li, N.W.; Lai, B. Efficient Degradation of Sulfamethoxazole by Acetylene Black Activated Peroxydisulfate. *Chin. Chem. Lett.* **2020**, *31*, 2657–2660. [CrossRef]
36. Lee, H.; Lee, H.J.; Jeong, J.; Lee, J.; Park, N.B.; Lee, C. Activation of Persulfates by Carbon Nanotubes: Oxidation of Organic Compounds by Nonradical Mechanism. *Chem. Eng. J.* **2015**, *266*, 28–33. [CrossRef]
37. Guan, C.T.; Jiang, J.; Luo, C.W.; Pang, S.Y.; Yang, Y.; Wang, Z.; Ma, J.; Yu, J.; Zhao, X. Oxidation of Bromophenols by Carbon Nanotube Activated Peroxymonosulfate (PMS) and Formation of Brominated Products: Comparison to Peroxydisulfate (PDS). *Chem. Eng. J.* **2018**, *337*, 40–50. [CrossRef]
38. Chen, S.H.; Ma, L.Y.; Du, Y.G.; Zhan, W.; Zhang, T.C.; Du, D.Y. Highly Efficient Degradation of Rhodamine B by Carbon Nanotubes-Activated Persulfate. *Sep. Purif. Technol.* **2021**, *256*, 117788. [CrossRef]
39. Ho, S.H.; Chen, Y.D.; Li, R.X.; Zhang, C.F.; Ge, Y.M.; Cao, G.L.; Ma, M.; Duan, X.G.; Wang, S.B.; Ren, N.Q. N-Doped Graphitic Biochars from C-Phycocyanin Extracted Spirulina Residue for Catalytic Persulfate Activation toward Nonradical Disinfection and Organic Oxidation. *Water Res.* **2019**, *159*, 77–86. [CrossRef]
40. Zhang, M.J.; Han, C.; Chen, W.Y.; Luo, W.; Cao, Y.Q.; Qian, G.; Zhou, X.G.; Duan, X.G.; Wang, S.B.; Duan, X.Z. Active Sites and Reaction Mechanism for N-Doped Carbocatalysis of Phenol Removal. *Green. Energy Environ.* **2020**, *5*, 444–452. [CrossRef]
41. Dippel, B.; Jander, H.; Heintzenberg, J. NIR FT Raman Spectroscopic Study of Flame Soot. *Phys. Chem. Chem. Phys.* **1999**, *1*, 4707–4712. [CrossRef]
42. Yan, J.; Gao, W.; Dong, M.; Han, L.; Qian, L.; Nathanail, C.P.; Chen, M. Degradation of Trichloroethylene by Activated Persulfate Using a Reduced Graphene Oxide Supported Magnetite Nanoparticle. *Chem. Eng. J.* **2016**, *295*, 309–316. [CrossRef]
43. Rasines, G.; Lavela, P.; Macias, C.; Zafra, M.C.; Tirado, J.L.; Parra, J.B.; Ania, C.O. N-doped Monolithic Carbon Aerogel Electrodes with Optimized Features for the Electrosorption of Ions. *Carbon* **2015**, *83*, 262–274. [CrossRef]
44. Di, J.; Zhu, M.; Jamakanga, R.; Gai, X.; Li, Y.; Yang, R. Electrochemical Activation Combined with Advanced Oxidation on $NiCo_2O_4$ Nanoarray Electrode for Decomposition of Rhodamine B. *J. Water Process Eng.* **2020**, *37*, 101386. [CrossRef]
45. Yang, S.J.; Guo, X.Y.; Wang, Z.R.; Dzakpasu, M.; Dai, X.F.; Ding, D.H.; Wu, K.; Huang, Y.; Zhang, Q.H.; Jin, P.K.; et al. Significance of B-Site Cobalt on Bisphenol A Degradation by MOFs-Templated $CoxFe_{3-x}O_4$ Catalysts and its Severe Attenuation by Excessive Cobalt-Rich Phase. *Chem. Eng. J.* **2019**, *359*, 552–563. [CrossRef]
46. Luo, R.; Li, M.Q.; Wang, C.H.; Zhang, M.; Khan, M.A.N.; Sun, X.Y.; Shen, J.Y.; Han, W.Q.; Wang, L.J.; Li, J.S. Singlet Oxygen-Dominated Non-Radical Oxidation Process for Efficient Degradation of Bisphenol A under High Salinity Condition. *Water Res.* **2019**, *148*, 416–424. [CrossRef] [PubMed]
47. Tang, M.; Zhang, Y. Enhancing the Activation of Persulfate Using Nitrogen-Doped Carbon Materials in the Electric Field for the Effective Removal of P-Nitrophenol. *RSC Adv.* **2021**, *11*, 38003–38015. [CrossRef] [PubMed]
48. Yun, E.T.; Lee, J.H.; Kim, J.; Park, H.D.; Lee, J. Identifying the Nonradical Mechanism in the Peroxymonosulfate Activation Process: Singlet Oxygenation Versus Mediated Electron Transfer. *Environ. Sci. Technol.* **2018**, *52*, 7032–7042. [CrossRef] [PubMed]
49. Li, J.J.; Cheng, X.W.; Zhang, H.X.; Gou, J.F.; Zhang, X.Y.; Wu, D.; Dionysiou, D.D. Insights into Performance and Mechanism of $ZnO/CuCo_2O_4$ Composite as Heterogeneous Photoactivator of Peroxymonosulfate for Enrofloxacin Degradation. *J. Hazard. Mater.* **2023**, *448*, 130946. [CrossRef]
50. Zhao, X.; Zhang, B.F.; Liu, H.J.; Chen, F.Y.; Li, A.Z.; Qu, J.H. Transformation Characteristics of Refractory Pollutants in Plugboard Wastewater by an Optimal Electrocoagulation and Electro-Fenton Process. *Chemosphere* **2012**, *87*, 631–636. [CrossRef]
51. Li, T.T.; Lu, S.; Lin, W.W.; Ren, H.J.; Zhou, R. Heat-Activated Persulfate Oxidative Degradation of Ofloxacin: Kinetics, Mechanisms, and Toxicity Assessment. *Chem. Eng. J.* **2022**, *433*, 133801. [CrossRef]

52. Hori, H.; Yamamoto, A.; Hayakawa, E.; Taniyasu, S.; Yamashita, N.; Kutsuna, S. Efficient Decomposition of Environmentally Persistent Perfluorocarboxylic Acids by Use of Persulfate as a Photochemical Oxidant. *Environ. Sci. Technol.* **2005**, *39*, 2383–2388. [CrossRef] [PubMed]
53. Liang, C.J.; Wang, Z.S.; Bruell, C.J. Influence of pH on Persulfate Oxidation of TCE at Ambient Temperatures. *Chemosphere* **2007**, *66*, 106–113. [CrossRef] [PubMed]
54. Guo, R.N.; Wang, Y.Y.; Li, J.J.; Cheng, X.W.; Dionysiou, D.D. Sulfamethoxazole Degradation by Visible Light Assisted Peroxymonosulfate Process Based on Nanohybrid Manganese Dioxide Incorporating Ferric Oxide. *Appl. Catal. B Environ.* **2020**, *278*, 119297. [CrossRef]
55. Liu, N.; Zhang, L.Y.; Xue, Y.; Lv, J.; Yu, Q.M.; Yuan, X.L. Nitrogen-Doped Carbon Material as a Catalyst for the Degradation of Direct Red23 Based on Persulfate Oxidation. *Sep. Purif. Technol.* **2017**, *184*, 213–219. [CrossRef]
56. Wang, Z.H.; Yuan, R.X.; Guo, Y.G.; Xu, L.; Liu, J.S. Effects of Chloride Ions on Bleaching of Azo Dyes by Co^{2+}/oxone Regent: Kinetic Analysis. *J. Hazard. Mater.* **2011**, *190*, 1083–1087. [CrossRef]
57. Bandala, E.R.; Pelaez, M.A.; Dionysiou, D.D.; Gelover, S.; Garcia, J.; Macias, D. Degradation of 2,4-Dichlorophenoxyacetic Acid (2,4-D) Using Cobalt-Peroxymonosulfate in Fenton-Like Process. *J. Photochem. Photobiol. A-Chem.* **2007**, *186*, 357–363. [CrossRef]

Disclaimer/Publisher's Note: The statements, opinions and data contained in all publications are solely those of the individual author(s) and contributor(s) and not of MDPI and/or the editor(s). MDPI and/or the editor(s) disclaim responsibility for any injury to people or property resulting from any ideas, methods, instructions or products referred to in the content.